Author's personal copy

Available online at www.sciencedirect.com
ScienceDirect
Physica A 387 (2008) 2293–2305
PHYSICA A
www.elsevier.com/locate/physa

Dynamic analysis of heartbeat rate signals of epileptics using multidimensional phase space reconstruction approach

Zhi-Yuan Su[a,*], Tzuyin Wu[b], Po-Hua Yang[c], Yeng-Tseng Wang[c]

[a] *Department of Information Management, Chia Nan University of Pharmacy & Science, Tainan 717, Taiwan*
[b] *Department of Mechanical Engineering, National Taiwan University, Taipei 106, Taiwan*
[c] *National Center for High-performance Computing, Tainan 742, Taiwan*

Received 11 May 2007; received in revised form 4 December 2007
Available online 14 December 2007

Abstract

The heartbeat rate signal provides an invaluable means of assessing the sympathetic–parasympathetic balance of the human autonomic nervous system and thus represents an ideal diagnostic mechanism for detecting a variety of disorders such as epilepsy, cardiac disease and so forth. The current study analyses the dynamics of the heartbeat rate signal of known epilepsy sufferers in order to obtain a detailed understanding of the heart rate pattern during a seizure event. In the proposed approach, the ECG signals are converted into heartbeat rate signals and the embedology theorem is then used to construct the corresponding multidimensional phase space. The dynamics of the heartbeat rate signal are then analyzed before, during and after an epileptic seizure by examining the maximum Lyapunov exponent and the correlation dimension of the attractors in the reconstructed phase space. In general, the results reveal that the heartbeat rate signal transits from an aperiodic, highly-complex behaviour before an epileptic seizure to a low dimensional chaotic motion during the seizure event. Following the seizure, the signal trajectories return to a highly-complex state, and the complex signal patterns associated with normal physiological conditions reappear.
© 2008 Elsevier B.V. All rights reserved.

Keywords: Chaos; Epilepsy; Nonlinearity; Phase space reconstruction; Correlation dimension

1. Introduction

Glass and Mackey [1] reported that the dynamics of a normal healthy biological system are chaotic, whereas those of a diseased system exhibit a more regular rhythmic behavior. Hence, the potential exists for performing disease diagnosis by monitoring the dynamics of the human body and its organs. However, for reasons as yet not fully clear, the heartbeat rate of even healthy human beings varies considerably, and thus interpreting the physiological and pathological implications of the heartbeat rate signal is highly challenging. Modeling human physiological systems mathematically based on empirical data acquired from experimental observations is fraught with difficulties since most experimental systems are capable of observing no more than a very limited number of physical responses (often just one). Fortunately, this problem can be overcome to a certain extent by employing time-series analysis methods

* Corresponding author. Tel.: +886 6 2664911x5305; fax: +886 6 3660607.
E-mail address: zysu@mail.chna.edu.tw (Z.-Y. Su).

0378-4371/$ - see front matter © 2008 Elsevier B.V. All rights reserved.
doi:10.1016/j.physa.2007.12.008

Author's personal copy

designed to extract the dynamics of nonlinear systems. Packard et al. [2] embedded a single scalar time series in a finite-dimensional phase-space picture and then analyzed its dynamics by determining its invariant properties. Takens [3] and Casdagli et al. [4] developed this embedding technique and proposed a formal embedology theorem laying down a set of guidelines for embedding time series into higher-dimensional phase spaces in order to support such applications as strange attractor detection in turbulent systems, time series prediction, and so forth. Importantly, the dynamics of the multidimensional phase space constructed from the time series data retain the essential dynamic characteristics of the original time series. In other words, the geometrical and dynamic properties of the phase space are equivalent to those of the original system, and thus, by applying appropriate unfolding techniques to the multidimensional phase space, the dynamics of the original system can be systematically explored.

Epilepsy is a brain disorder in which neurons in the brain signal abnormally, causing the sufferer to experience strange sensations and emotions, physical seizures, or even a loss of consciousness. Although epilepsy is conventionally diagnosed by performing electroencephalogram (EEG) tests or brain scans, the use of electrocardiogram (ECG) tests, in which the rate and regularity of the heartbeat are measured over time, also represents a potential diagnostic technique since it has been shown that epileptic seizures are frequently accompanied by a significant increase in the rate of the heartbeat [5,6]. However, a review of the literature reveals that the dynamic characteristics of the heartbeat rate signal before, during and after an epileptic seizure have received little attention.

Rosen [7] demonstrated the feasibility of using conventional dynamic system theory to clarify the complex oscillations of biological systems in both a qualitative and a quantitative manner. The present study applies the embedology theorem to construct multidimensional phase spaces corresponding to the heartbeat rate signals of known epilepsy sufferers and then applies conventional dynamic analysis tools (i.e. the Lyapunov exponent and the correlation dimension) to analyze the dynamics of the heartbeat rate signal before, during and after an epileptic event. The present investigations aim principally to provide a deeper understanding of the electrical activity of the heart in known epilepsy sufferers in order to support the epilepsy diagnostic process. However, the analytical technique presented in this study also has a wider application to the diagnosis of cardiac disorders associated with heart disease or aging since it has been reported that such disorders are frequently associated with a decrease of cardiac chaos [8,9].

2. Nonlinear dynamic analysis

2.1. Phase space reconstruction

The equation describing the heartbeat rate is unknown and hence the dynamics of the heartbeat signal can not be directly determined. Accordingly, in this study, the embedology theorem [3,4] is used to construct a multidimensional phase space from the one-dimensional time series representing the heartbeat activity. The dynamics of the heartbeat rate signal are then examined using conventional dynamic systems analysis techniques. The basic principles of the phase space construction process are described below.

Assume that the dynamic system of interest is given by

$$\vec{x}(n) \to \vec{F}(\vec{x}(n)) = \vec{x}(n+1). \tag{1}$$

If the variable $\vec{x}$ and action function $\vec{F}$ of this dynamic system are unknown, only the scalar value $h(\bullet)$ can be measured. The relationship between $h(\bullet)$ and $\vec{x}$ is described by the unknown function $h(\vec{g}(\vec{x}(n)))$. According to the embedology theorem, the trajectory of the dynamic system in the original phase space can be unfolded using the vector $\vec{y}(n)$, constructed from the scalar value $h(\bullet)$ as follows:

$$\vec{y}(n) = [h(\vec{x}(n)), h(\vec{g}^{T_1}(\vec{x}(n))), h(\vec{g}^{T_2}(\vec{x}(n))), \ldots, h(\vec{g}^{T_{d-1}}(\vec{x}(n)))]. \tag{2}$$

The space in which the vector $\vec{y}(n)$ is located is known as the reconstructed phase space, and its dimension d is referred to as the embedding dimension. For dynamic systems, the most convenient scalar value, $h(\bullet)$, is the experimentally measured time series $s(n)$, i.e.

$$h(\vec{x}(n)) = s(n). \tag{3}$$

Author's personal copy

The vector function $\vec{g}(\vec{x})$ can usually be expressed in the form of a time delay function, i.e.

$$\vec{g}^{\,T_k}(\vec{x}(n)) = \vec{x}(n + T_k). \tag{4}$$

Therefore, the vector $\vec{y}(n)$ can be rewritten as

$$\vec{y}(n) = [s(n), s(n + T_1), s(n + T_2), \ldots, s(n + T_{d-1})]. \tag{5}$$

For convenience, T_k is selected as a multiple of the time delay T, i.e. $T_k = kT$. As a result, $\vec{y}(n)$ can be further expressed as

$$\vec{y}(n) = [s(n), s(n + T), s(n + 2T), \ldots, s(n + (d - 1)T)]. \tag{6}$$

According to the embedology theorem, the trajectories $\vec{y}(n)$ in the d-dimension of the reconstructed phase space have similar behavioural characteristics to those within the original phase space.

2.2. Selection of time lag using average mutual information method

The phase space reconstruction process requires the selection of an appropriate time lag T. In this study, the appropriate value of the time lag is determined using the average mutual information method proposed by Fraser and Swinney [10].

Assume that an experiment yields two measured values, i.e. a_i and b_i, and that all possible values of a_i and b_i congregate into two sets, namely $A = \{a_i\}$ and $B = \{b_i\}$. The average mutual information of the data in these two sets can be defined as

$$I_{AB} = \sum_{a_i, b_j} P_{AB}(a_i, b_j) \log_2 \left[\frac{P_{AB}(a_i, b_j)}{P_A(a_i) P_B(b_j)} \right], \tag{7}$$

where P_{AB} indicates the joint probability distribution function of A and B, while P_A and P_B represent the marginal probability functions of A and B respectively.

In the current context, set A can be regarded as containing the values of $s(n)$ observed at time n, while set B represents the values of $s(n)$ after the time delay, T. Hence, the average mutual information between $s(n)$ and $s(n+T)$ is given by

$$I(T) = \sum_{s(n), s(n+T)} P(s(n), s(n + T)) \log_2 \left[\frac{P(s(n), s(n + T))}{P(s(n)) P(s(n + T))} \right]. \tag{8}$$

In most cases $I(T) \geq 0$. Note that for the particular case of $T = 0$, $I(T)$ is equivalent to the entropy of the system.

2.3. Global false nearest neighbours

Having specified the time delay T, an appropriate embedding dimension d should be selected for the reconstructed phase space. In the current study, this is achieved using the false nearest neighbours (FNN) approach presented by Kennel et al. [11]. Suppose that a point located in the d-dimensional reconstructed space is described by

$$\vec{y}(n) = [s(n), s(n + T), \ldots, s(n + (d - 1)T)]. \tag{9}$$

The nearest neighbour to this point, i.e. the point which lies at the shortest distance from $\vec{y}(n)$, is given by

$$\vec{y}^{\,NN}(m) = [s^{NN}(m), s^{NN}(m + T), \ldots, s^{NN}(m + (d - 1)T)], \tag{10}$$

where m denotes the "nearest neighbour" point and n is the original point.

Author's personal copy

However, point $\vec{y}^{NN}(m)$ may be a false nearest neighbour arising from a higher-dimension projection. This can be checked by calculating the distance $R_d(n, m)$ between points $\vec{y}(n)$ and $\vec{y}^{NN}(m)$ under dimension d.

$$R_d^2(n, m) = \sum_{k=1}^{d} [s(n + (k-1)T) - s^{NN}(m + (k-1)T)]^2. \tag{11}$$

When the dimension is unfolding to $d + 1$, the distance between the two points becomes

$$\begin{aligned} R_{d+1}^2(n, m) &= \sum_{k=1}^{d+1} [s(n + (k-1)T) - s^{NN}(m + (k-1)T)] \\ &= R_d^2(n, m) + |s(n + \mathrm{d}T) - s^{NN}(m + \mathrm{d}T)|^2. \end{aligned} \tag{12}$$

The difference between the two distances can be quantified as follows:

$$\sqrt{\frac{R_{d+1}^2(n, m) - R_d^2(n, m)}{R_d^2(n, m)}} = \frac{|s(n + \mathrm{d}T) - s^{NN}(m + \mathrm{d}T)|}{R_d(n, m)}. \tag{13}$$

If the result exceeds a predetermined value R_{tol}, then $\vec{y}^{NN}(m)$ is a false nearest neighbour of $\vec{y}(n)$. In most general applications, R_{tol} is assigned a value of 15. The procedure described above is repeated for all neighboring points in the d-dimension space. The dimension number is then increased to $d + 1$, and the verification procedure is repeated. This process continues iteratively until the proportion of false nearest neighbours reduces to zero, indicating that an appropriate dimension has been found.

2.4. The Lyapunov exponent

Having established appropriate values of the time delay T and the embedding dimension d, the time series $s(n)$ can be transformed into the corresponding trajectories $\vec{y}(n)$ in the reconstructed phase space. The dynamic behaviour of the original system can then be explored by examining the invariant properties of $\vec{y}(n)$. One of the most important invariant properties is the Lyapunov exponent, λ, which quantifies the divergence rate of nearby trajectories and is given by

$$|\vec{x}_1(t') - \vec{x}_2(t')| \approx |\vec{x}_1(t) - \vec{x}_2(t)| \mathrm{e}^{\lambda |t' - t|}. \tag{14}$$

In Eq. (14), a positive Lyapunov exponent indicates the existence of chaotic motion. In the current study, the dynamics of the heartbeat rate signal are analysed by computing the maximum Lyapunov exponent value using the method presented by Wolf et al. [12].

2.5. Correlation dimension of heartbeat rate signal

In the current analysis, the dynamics of the heartbeat rate signal are also examined by determining the correlation dimension using the algorithm presented by Grassberger and Procaccia [13]. In general, if N points are selected within an attractor, the probability that the other $N - 1$ points fall within a radius R centred at the ith point in the phase space is denoted by $p_i(R)$. The correlation sum $C(R)$ can then be defined as

$$C(R) = \frac{1}{N} \sum_{i=1}^{N} p_i(R). \tag{15}$$

The correlation dimension D_c is given by the log ratio of $C(R)$ to R as the value of R approaches 0, i.e.

$$D_c = \lim_{R \to 0} \frac{\log C(R)}{\log R}. \tag{16}$$

Author's personal copy

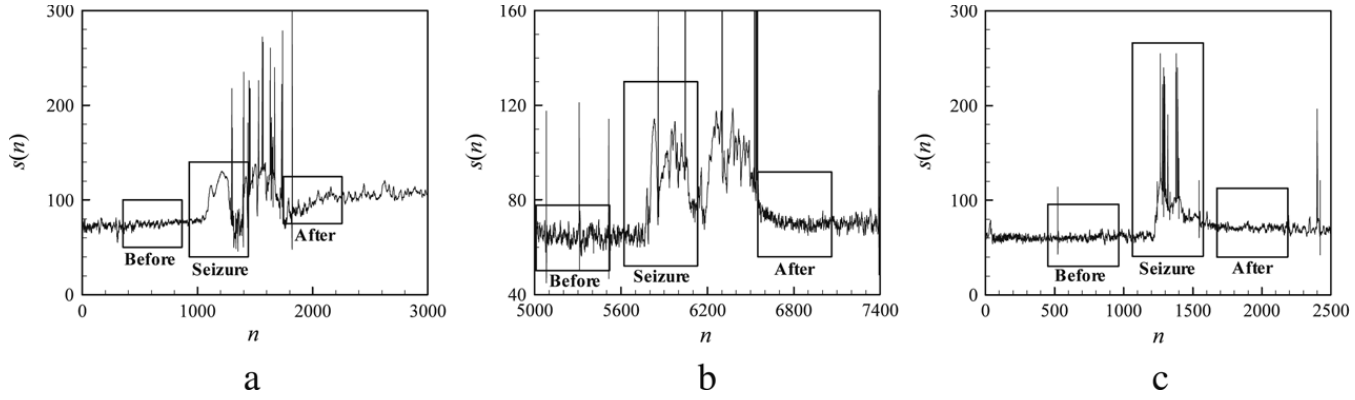

Fig. 1. Time series corresponding to heartbeat rate signals of: (a) subject 1; (b) subject 2; and (c) subject 3.

In general, D_c is not necessarily an integer. In the event that D_c is a fraction, the geometrical structure of the attractor is said to be "fractal".

3. Power spectrum and autocorrelation analyses of epileptic heartbeat rate

3.1. Data acquisition

The heartbeat rate data examined in the current study are taken from the "Post-Ictal Heart Rate Oscillations in Partial Epilepsy" pattern archived in the PhysioBank ECG Database [14]. The data were originally acquired by Al-Aweel et al. [15] from a group of five female patients aged between 31 and 48 with partial epilepsy but no clinical evidence of cardiac disease. The data were gathered via EEG/ECG/video monitoring using a protocol approved by the Beth Israel Deaconess Medical Center Committee on Clinical Investigations and were then transformed into a time series format.

3.2. Data selection

Fig. 1 presents the time series of the heartbeat rate signals of three of the five patients. The time series shown in Fig. 1(a) comprises a total of 8384 discrete data points, of which those between 352 and 863 represent pre-seizure data points, while those between 928 and 1439 represent seizure data points, and those between 1744 and 2255 represent post-seizure data points. Similarly, in Fig. 1(b), corresponding to the second patient, the time series has a total of 16 383 points, of which those between 5009 and 5520, 5620 and 6131, and 6550 and 7061 correspond to preseizure, seizure and postseizure data points, respectively. Finally, the time series for the third patient, shown in Fig. 1(c), contains a total of 6228 points, of which those between 452 and 963, 1063 and 1574, and 1674 and 2185 are preseizure, seizure and postseizure points, respectively. Note that in every case, the heartbeat rate samples have a length of 512 data points. The current analysis procedure commenced by conducting power spectrum and autocorrelation analyses of each data sample. Many commercial numerical software packages provide subroutines for performing such analyses. In the current study, the analyses were performed using MATLAB software.

3.3. Power spectrum analysis

Fig. 2(a) shows the power spectra of the time series corresponding to the heartbeat rate of the first subject. It can be seen that prior to the seizure, prominent power peaks occur at a frequency of 0.02 Hz, and to a lesser degree at 0.25 Hz, the frequency corresponding to respiration. During seizure, the power spectrum exhibits a sharp energy peak in the low-frequency region (<0.05 Hz), but has a lower energy distribution at all other frequencies. Such a spectrum is characteristic of a system performing periodic or pseudo-periodic motion. Following the seizure event, the spectrum not only has a high energy distribution at low frequencies, but also exhibits a relatively high energy level over the remaining frequency range. Comparing the pre- and post-seizure results, it can be seen that the sharp spectral peak in the low-frequency region of the post-seizure spectrum has a significantly greater amplitude than that in the preseizure spectrum. Moreover, the energy peak observed at 0.25 Hz in the preseizure spectrum is not obvious in

Author's personal copy

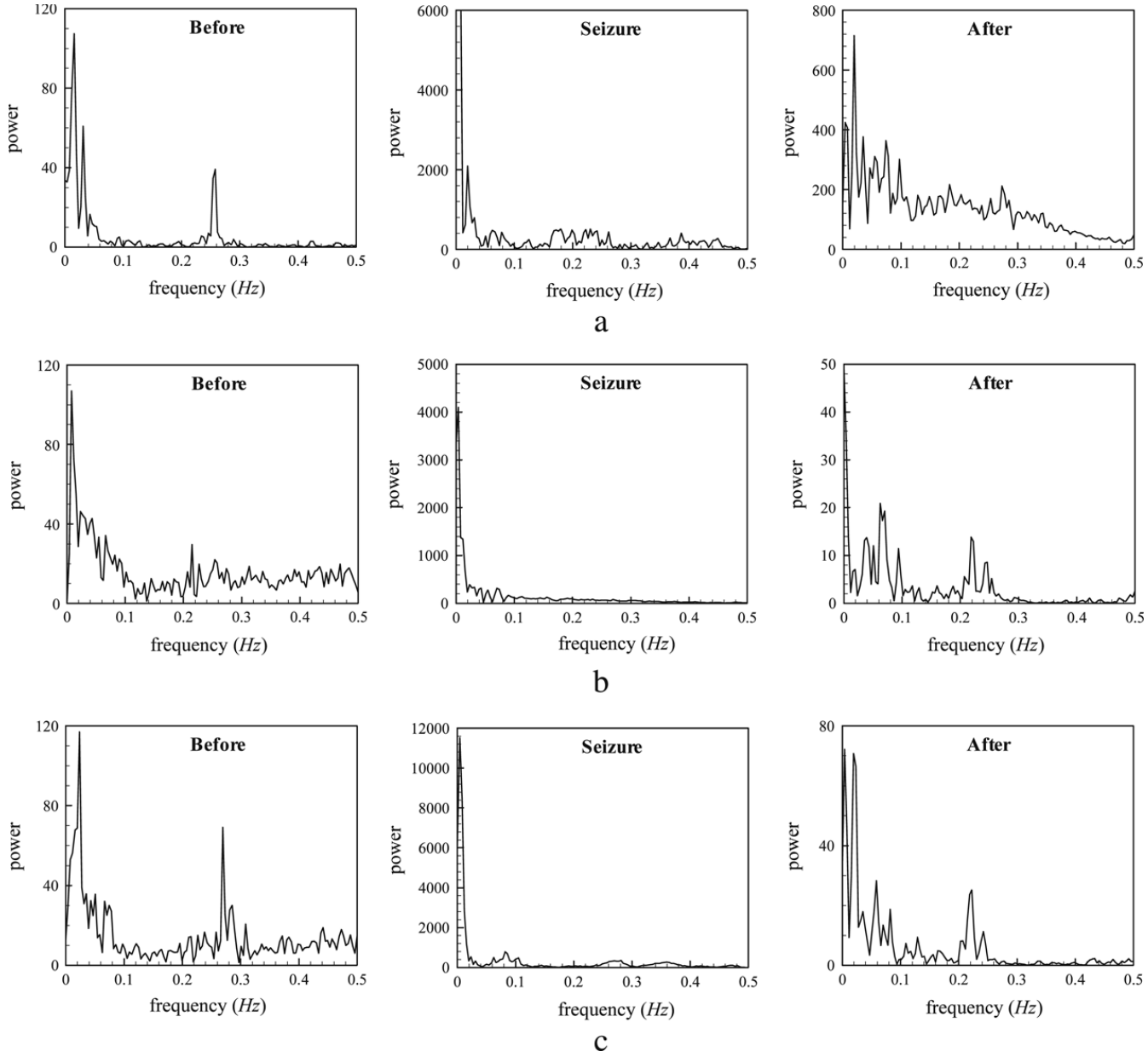

Fig. 2. Power spectra of heartbeat rate signals before, during and after epileptic seizure of: (a) subject 1; (b) subject 2; and (c) subject 3.

the post-seizure spectrum. The power spectra for the second subject are shown in Fig. 2(b), and are notably different from those of the first. For example, the energy distribution before seizure is both broader and more continuous than that observed in Fig. 2(a). The major energy peaks occur at frequencies of approximately 0.02 Hz and 0.22 Hz, respectively, where the latter peak coincides with the typical frequency of respiration. During seizure, it can be seen that a sharp energy peak appears in the very low-frequency region, but the energy is otherwise insignificant over most of the remaining frequency range. Finally, following the seizure, the total energy is confined primarily to the frequency range of 0–0.3 Hz, with the bulk of this energy concentrated at frequencies lower than 0.1 Hz. The results presented in Fig. 2(c) for the third subject are similar to those presented in Fig. 2(b) other than a more prominent energy peak at the frequency corresponding to respiration prior to seizure and a higher peak amplitude at a frequency of around 0.02 Hz both during and after the seizure.

Overall, the power spectra presented in Fig. 2 show that during an epileptic seizure, the power of the heartbeat rate signal is concentrated in a very narrow band of less than 0.05 Hz. However, before and after the seizure event, the power is spread over a far wider frequency range. This observation is consistent with the findings presented by Das et al. [16] regarding the relationship between the signal bandwidth and the dimension of a chaotic system. The slightly

Author's personal copy

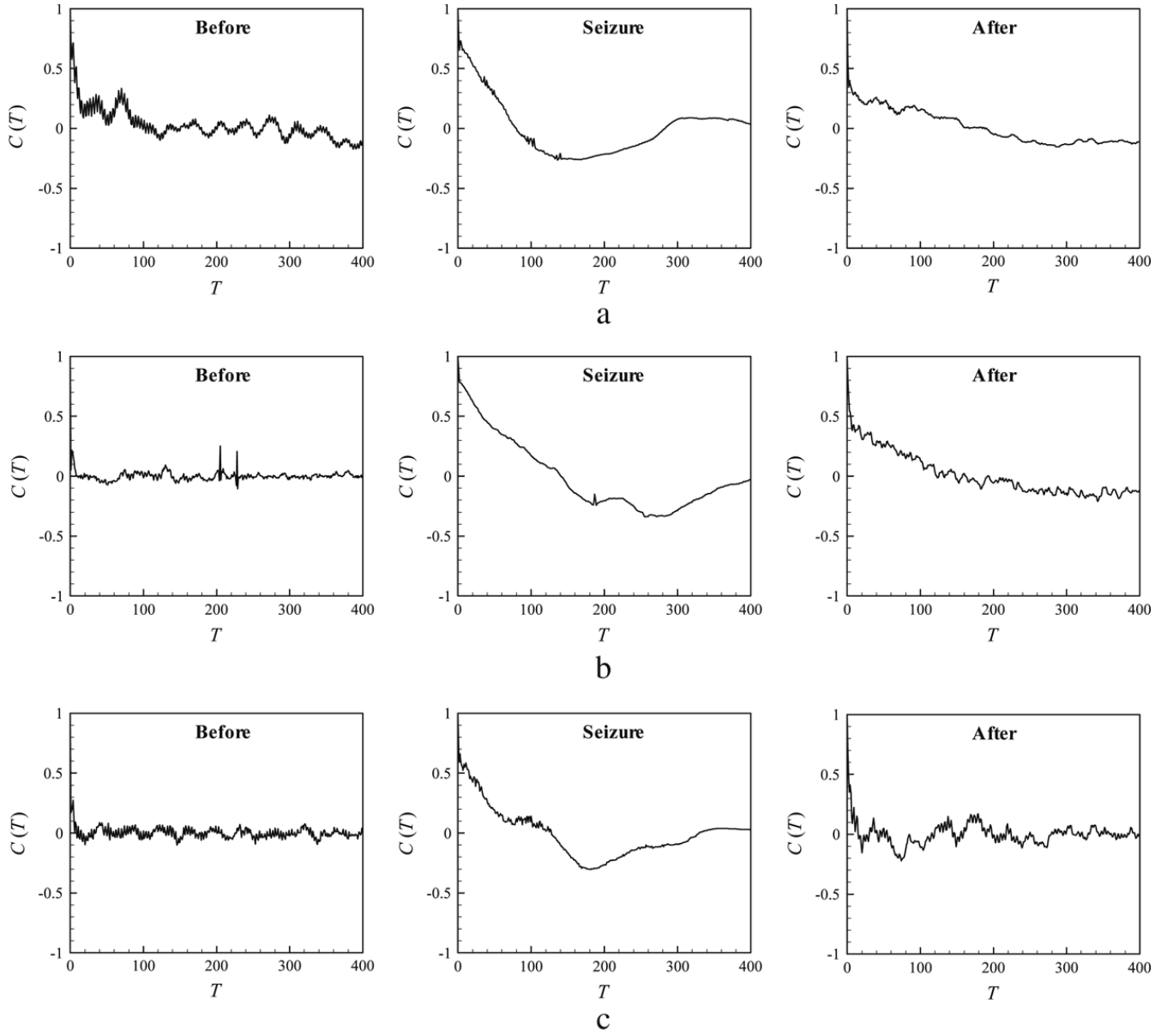

Fig. 3. Autocorrelation functions of heartbeat rate signals before, during and after epileptic seizure of: (a) subject 1; (b) subject 2; and (c) subject 3.

different tendencies of the power spectra shown in Fig. 2(a) compared to those in Fig. 2(b) and (c), respectively, may well be a result of differences in the physical conditions of the three patients. For example, the first patient may possess different area's brain function disorder.

3.4. Autocorrelation analysis

The autocorrelation function is defined as $C(T) = \lim_{T\to\infty} \int_0^T s(n)s(n+T)\mathrm{d}n$. For the particular case of $T = 0$, $C(T)$ is equivalent to the power of $s(n)$. However, when $T \neq 0$, $C(T)$ provides an indication of the relationship between the data value at one moment in time and the data value following an elapsed time equal to T. If the signal has the form of white noise, the data values at the two points in time have no correlation with one another. However, if the signal has a periodic characteristic, the corresponding autocorrelation function is also periodic.

Fig. 3(a)–(c) show the autocorrelation functions for the heartbeat rate signals presented in Fig. 1. In general, it can be seen that in all three sets of figures, the autocorrelation function has a slow decaying tendency characterized by a few minor oscillations during the seizure event. For the first subject, the autocorrelation function falls to a

Author's personal copy

Table 1
Time delay parameters used in reconstruction of phase spaces of heartbeat rate signals before, during and after epileptic seizure

	Before	During	After
Subject 1	2	11	9
Subject 2	9	10	2
Subject 3	2	7	3

value of zero at around $T = 80$ and remains at this level to around $T = 160$, at which point it starts to gradually increase. Meanwhile, for the second subject, the autocorrelation function falls to zero at $T = 140$ and begins to increase at around $T = 280$. Finally, for the third patient, the autocorrelation falls to zero at around $T = 125$ and begins to increase at $T = 180$. Observing Fig. 3(b) and (c), it can be seen that for the second and third subjects, the autocorrelation function of the heartbeat rate signal prior to seizure falls to zero virtually immediately, and then oscillates around this value for the remainder of the sampled period. This result suggests the presence of a random heartbeat rate signal in the preseizure period. A similar trend is noted in the autocorrelation function of the heartbeat rate signal of the third subject after the seizure event. However, the autocorrelation function decays far more slowly in the case of the signal associated with the second subject after the seizure event. Finally, inspecting the results corresponding to the first subject, it can be seen that the autocorrelation function decays slowly to zero both before and after the seizure event, which almost certainly implies the presence of a relatively regular signal pattern than the second and third subjects.

4. Phase space reconstruction of epileptic heartbeat rate

The power spectrum and autocorrelation analyses presented in the previous section provide basic insights into the characteristics of the heartbeat rate signal of epileptic patients. However, they do not provide a full and reliable indication of the detailed dynamics of the underlying nonlinear system. In general, the dynamics of the heartbeat rate signal are governed by many variables, and thus it is impractical to simulate their characteristics using mathematical models. However, as discussed previously, this problem can be resolved by using the embedology theorem to project the one-dimensional nonlinear heartbeat signal into a multidimensional phase space and then using conventional dynamic analysis techniques to explore the dynamic characteristics of the resulting attractor. Phase space reconstruction requires the use of two parameters, namely the time delay T and the embedding dimension d. As described earlier, in the current study, these parameters are derived using the average mutual information method and the FNN technique, respectively.

4.1. Average mutual information

Eq. (8) can be processed repeatedly for various values of the time delay T to generate a curve describing the relationship between $I(T)$ and T. According to the average mutual information method, the value of the time delay parameter required to construct the multidimensional phase space is given by the value of T corresponding to the first local minimum in the $I(T)$ vs. T curve. Table 1 summarizes the corresponding time delay values before, during and after the seizure event for each of the three subjects considered in the present study.

4.2. Global false nearest neighbours

The appropriate embedding dimensions for reconstructing the phase spaces of the three heartbeat rate signals considered in this study are determined by systematically computing the proportion of false nearest neighbours (FNNs) in each time series for different numbers of unfolding dimensions. In practice, the heartbeat rate data inevitably contains noise, and thus the FNN proportion can never reduce precisely to zero irrespective of the number of dimensions considered. Accordingly, in this study, the embedding dimensions for the heartbeat rate signals are specified as the values of d at which the FNN metric converges to a discernible minimum value. Table 2 summarizes the results obtained for the appropriate embedding dimensions for the heartbeat rate signals before, during and after the seizure event for each of the three subjects.

Author's personal copy

Table 2
Embedding dimension parameters used in reconstruction of phase spaces of heartbeat rate signals before, during and after epileptic seizure

	Before	During	After
Subject 1	3	3	4
Subject 2	4	4	3
Subject 3	2	3	3

Table 2 shows that when reconstructing a multidimensional phase space for the heartbeat rate signals of epileptic patients, the number of dimensions required ranges from 2 to 4. Although the embedding dimension is induced from geometrical concepts (i.e. the FNN approach, in the current case), its value is not necessarily equal to the actual dimension (i.e. degrees of freedom) of the original system. Nevertheless, the embedding dimension calculated from a one-dimensional time series provides an approximate indication of the probable number of variables influencing the time series.

4.3. Trajectory behaviour in three-dimensional phase space

Having determined the appropriate embedding dimensions and time delay, a reconstructed attractor can be generated from the one-dimensional time series in the corresponding multidimensional phase space. Although the trace of the heartbeat rate signal in the reconstructed phase space differs from that in the original phase space, according to the embedology theorem, the original and reconstructed phase spaces have identical geometrical characteristics and dynamic behaviours. As shown in Table 2, some of the reconstructed phase spaces for the current heartbeat rate time series require more than three dimensions. Reproducing a system with more than three dimensions on a flat page is difficult, and hence in the current study, the projection of the attractor is shown in a three-dimensional space spanned by time-delay coordinates. Fig. 4(a)–(c) show the trajectories of the three subjects' heartbeat rates before, during and after an epileptic seizure. In general, the figures show that the signal trajectories before the seizure are highly chaotic, i.e. they have the appearance of randomly scribbled lines with no obvious pattern. In other words, the attractor has an aperiodic nature before the seizure event. However, during the seizure, the trajectories are less chaotic, and exhibit a more regular motion. Thus, it can be inferred that the signals have a more periodic type characteristic. Finally, after the seizure event, the signal trajectories return to a chaotic state, and the complex signal patterns associated with normal physiological conditions reappear. In general, the results presented in Fig. 4 are consistent with the findings of Shafferet al. [17], who reported that during an epileptic seizure, the trajectory of the EEG signal approaches a transient periodicity, but then recovers to a more chaotic mode once the seizure has passed.

4.4. The Lyapunov exponent

The Lyapunov exponent, λ, is one of the most important invariant properties and is used to quantify the divergence rate of nearby trajectories. A positive Lyapunov exponent indicates the presence of chaotic motion. Table 3 summarizes the maximum λ values obtained from calculations performed using the time delay and embedding dimension data presented in Tables 1 and 2, respectively. It can be seen that for every patient, the Lyapunov exponent has a positive value before, during and after the seizure, indicating that the heartbeat rate signal has a consistently chaotic characteristic. However, during the epileptic seizure, it is observed that the value of λ reduces. Consequently, it can be inferred that the trace's speed of dissipation is slightly slower than before or after the epileptic seizure. This may well explain why the trace movement structure of heartbeat rate signals during an epileptic seizure has the form of a limited circle in three-dimensional space. In other words, from a dynamic perspective, the onset of a seizure represents a transition from a complex to a more ordered state.

The literature contains very little information regarding the use of nonlinear analysis techniques to analyse the heartbeat rate of epileptics, and thus it is difficult to provide a robust validation of the current results. However, the results are in good agreement with the dynamic analysis data presented by Iasemidis and Sackellares [18,19] for the EEG recordings of epilepsy patients. In their studies, the authors showed that the dynamic properties of the preictal, ictal and postictal states of the heartbeat rate signal in temporal lobe epilepsy patients were distinctly different. Specifically, they observed that the signal chaos (as indicated by the value of the maximum Lyapunov exponent) fell to its lowest level during the actual seizure discharge.

Author's personal copy

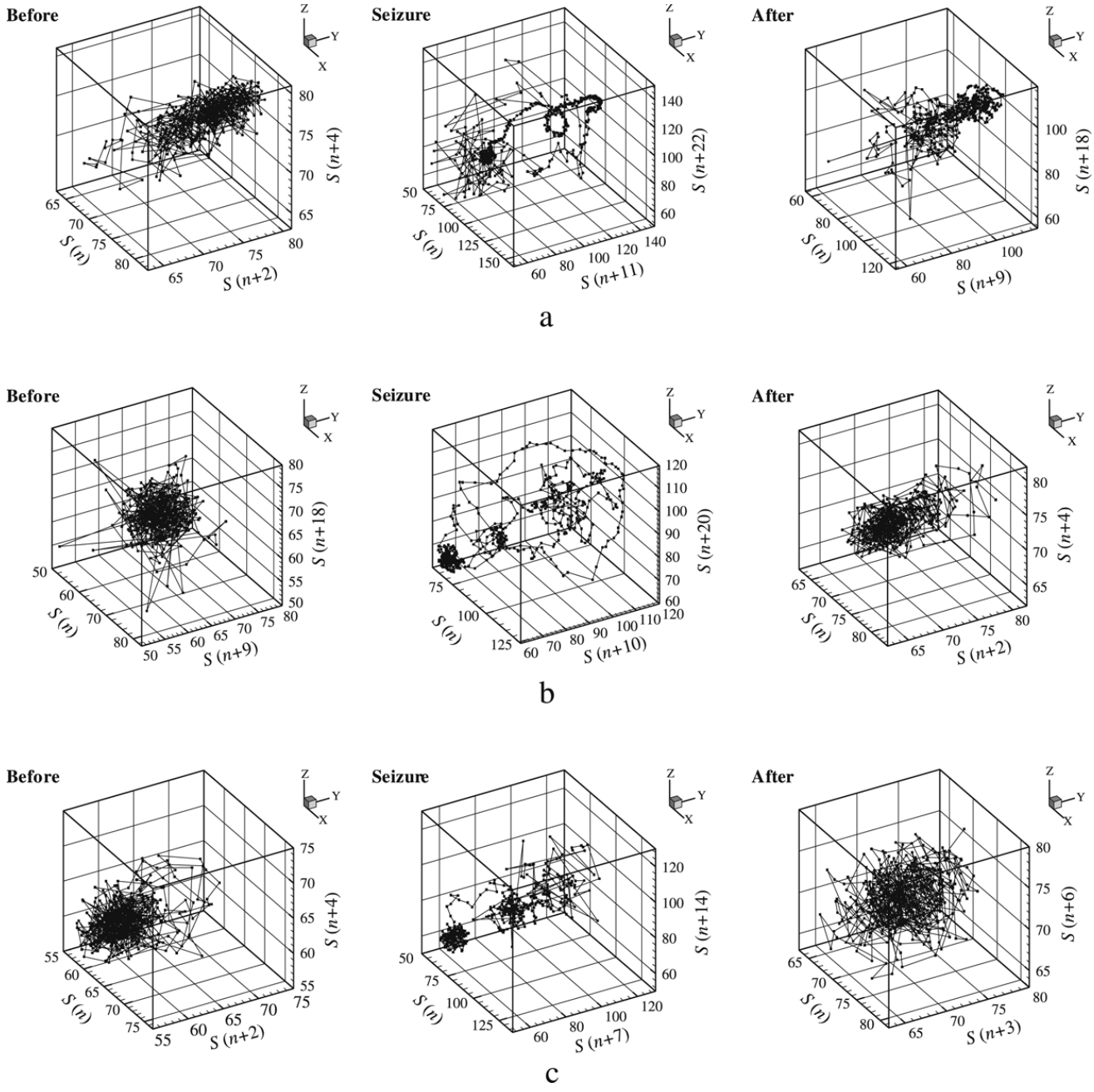

Fig. 4. Three-dimensional phase space representations of heartbeat rate signals before, during and after epileptic seizure of: (a) subject 1; (b) subject 2; and (c) subject 3.

Table 3
Lyapunov exponents before, during and after epileptic seizure

	Before	During	After
Subject 1	0.758	0.206	0.432
Subject 2	0.234	0.125	0.383
Subject 3	0.511	0.166	0.215

4.5. The correlation dimension

Further insights into the dynamics of the heartbeat rate signals can be obtained by examining the correlation dimension quantity. As described earlier, in the current study, the correlation dimension is computed using the

Author's personal copy

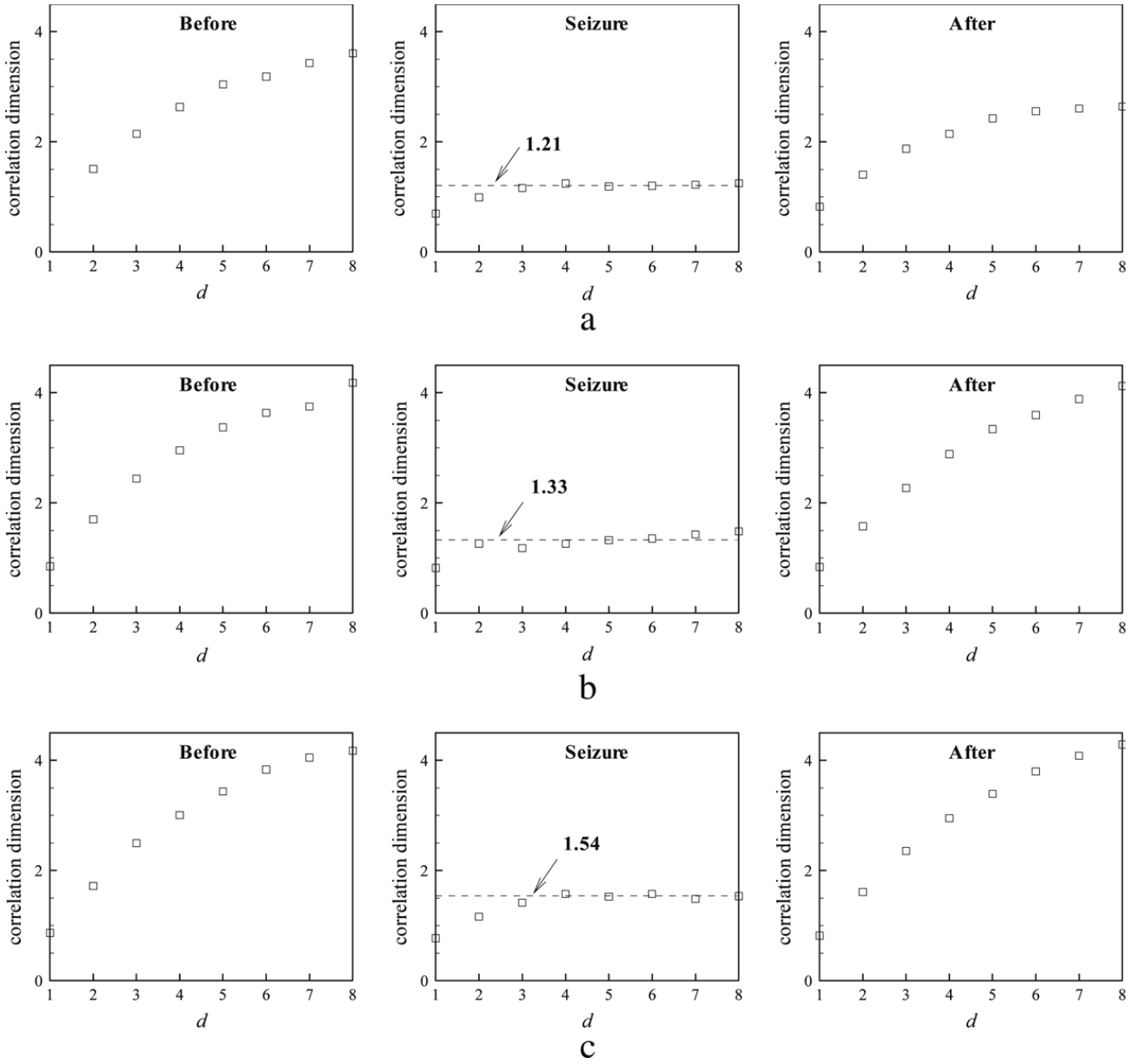

Fig. 5. Correlation dimensions of heartbeat rate signals before, during and after epileptic seizure of: (a) subject 1; (b) subject 2; and (c) subject 3.

algorithm developed by Grassberger and Procaccia [13]. Fig. 5 presents the variation of the correlation dimension with the embedding dimension before, during and after the seizure for each of the three subjects. In general, when a time series is unfolded into trajectories in phase spaces with different numbers of dimensions, the correlation dimension increases with the embedding dimension number. At a certain dimension, however, the correlation dimension becomes saturated and remains constant. Fig. 5 shows that the correlation dimension of the heartbeat rate signal before and after the epileptic seizure increases along the 45-deg line. Therefore, it can be inferred that the heartbeat rate signal has a very high degree of freedom before and after a seizure event. This result is consistent with the findings of Theiler et al. [20], who utilized a surrogate data approach for identifying brain wave nonlinearity and found that the estimated dimension increases almost as rapidly with embedding dimension for the original time series. During the seizure event, the correlation dimension of the three signals saturates at a value between 1 and 2. The correlation dimension of the reconstructed attractor during seizure and the positive low value of the maximum Lyapunov exponent (see Table 3) suggest that the heartbeat rate signal is characterized by a low-dimensional chaotic motion. The results presented in Fig. 5 are consistent with those presented in the literature based upon dynamic analyses of the EEG recordings of epileptic subjects. For example, Pijn et al. [21] calculated the correlation dimension of EEG signals

Author's personal copy

recorded from different limbic cortex sites of a rat in various states, i.e. wakeful rest, locomotion and epileptic seizure. The results showed that the high dimensional signals in the first two states were indistinguishable from random noise. However, during an epileptic seizure, the correlation dimension reduced to a very low level. Meanwhile, Lehnertz and Elger [22] performed a correlation dimension analysis of the EEG signals of twenty patients with unilateral temporal lobe epilepsy and found that a distinct reduction in the correlation dimension occurred during an epileptic seizure, with the most pronounced reduction taking place in the "zone of ictal onset". Finally, Silva et al. [23] reported that the chaotic dynamics of the EEG signal observed during a seizure are determined by a small number of variables and have a low complexity.

5. Conclusion

This study has employed the embedology theorem to construct multidimensional phase spaces corresponding to the heartbeat rate signals of epilepsy patients before, during and after an epileptic seizure. Having first obtained a basic understanding of the heartbeat characteristics by performing power spectrum and autocorrelation analyses, the detailed dynamic properties of the heartbeat rate signals have been analysed using the maximum Lyapunov exponent and the correlation dimension property. In general, the results have shown that the heartbeat rate signal exhibits a low-dimensional chaotic motion ($D_C \leq 2$) during the seizure event. This result is consistent with the Lyapunov exponent analysis, which has shown that during the seizure, the maximum Lyapunov exponent has a positive but low value. This indicates that the trajectory within the multiple-dimensional attractor has a chaos characteristic. Furthermore, the correlation dimension has a non-integer value during the seizure event, which implies that the attractor structure has a fractal characteristic. The dynamic analysis results have shown that the maximum Lyapunov exponents of the reconstructed trajectories prior to and following seizure are notably higher than those during the seizure event. Furthermore, the corresponding correlation dimension properties increase continuously with an increasing number of unfolding dimensions. As a result, the trajectories in the reconstructed phase space have a random, irregular appearance.

Overall, the present results reveal that the heartbeat rate signal changes from a complex, aperiodic behaviour before the seizure, to a low-dimensional chaotic state during the seizure itself, and then back to a highly complex behaviour following the seizure event. The results presented in this study demonstrate the feasibility of applying the embedology theorem and conventional nonlinear analysis techniques to characterize the dynamic behaviour of the heartbeat rate signals of epilepsy patients. Significantly, the proposed approach not only facilitates the diagnosis of epilepsy via the monitoring of ECG signals, but also supports the diagnosis of cardiac disorders associated with heart disease or aging.

References

[1] L. Glass, M.C. Mackey, From Clocks to Chaos: The Rhythms of Life, Princeton Univ. Press, Princeton, NJ, 1988.
[2] N.H. Packard, J.P. Crutchfield, J.D. Farmer, R.S. Shaw, Phys. Rev. Lett. 45 (1980) 712.
[3] F. Takens, Detecting Strange Attractors in Turbulence, in: D.A. Rand, L.S. Young (Eds.), Dynamical Systems and Turbulence, Springer-Verlag, Berlin, 1981.
[4] M. Casdagli, T. Sauer, J.A. Yorke, J. Stat. Phys. 65 (1991) 579.
[5] C.A. Galimberti, E. Marchioni, F. Barzizza, R. Manni, I. Sartori, A. Tartara, Epilepsia 37 (1996) 742.
[6] R.C. Frysinger, R.M. Harper, Epilepsia 31 (1990) 162.
[7] R. Rosen, Dynamical System Theory in Biology, Volume I: Stability Theory and Its Applications, Wiley-Interscience, New York, 1970.
[8] A.L. Goldberger, V. Bhargava, B.J. West, A.J. Mandell, Physica D 19 (1986) 282.
[9] A.L. Goldberger, News Physiol. Sci. 6 (1991) 87.
[10] A.M. Fraser, H.L. Swinney, Phys. Rev. A 33 (1986) 1134.
[11] M.B. Kennel, R. Brown, H.D.I. Abarbanel, Phys. Rev. A 45 (1992) 3403.
[12] A. Wolf, J.B. Swift, H.L. Swinney, J.A. Vastano, Physica D 16 (1985) 285.
[13] P. Grassberger, I. Procaccia, Phys. Rev. Lett. 50 (1983) 346.
[14] A.L. Goldberger, L.A.N. Amaral, L. Glass, J.M. Hausdorff, P.Ch. Ivanov, R.G. Mark, J.E. Mietus, G.B. Moody, C.K. Peng, H.E. Stanley, Circulation 101 (2000) e215.
[15] I.C. Al-Aweel, K.B. Krishnamurthy, J.M. Hausdorff, J.E. Mietus, J.R. Ives, A.S. Blum, D.L. Schomer, A.L. Goldberger, Neurology 53 (1999) 1590.
[16] B. Das, A.M. Albano, N.B. Abraham, Phys. Rev. A 41 (1990) 6162.
[17] W.M. Schaffer, B. Kendall, C.W. Tidd, L.F. Olsen, IMA J. Math. Appl. Med. Biol. 10 (1993) 227.
[18] L.D. Lasemidis, J.C. Sackellares, H.P. Zaveri, W.J. Williams, Brain Topogr. 2 (1990) 187.
[19] L.D. Lasemidis, J.C. Sackellares, The Neuroscientist 2 (1996) 118.

Author's personal copy

[20] J. Theiler, S. Eubank, A. Longtin, B. Galdrikian, J.D. Farmer, Physica D 58 (1992) 77.
[21] J.P. Pijn, J. Vanneerven, A. Noest, F.H.L. Dasilva, Electroencephalogr. Clin. Neurophysiol. 79 (1991) 371.
[22] K. Lehnertz, C.E. Elger, Electroenceph. Clin. Neurophysiol. 95 (1995) 108.
[23] C. Silva, I.R. Pimentel, A. Andrade, J.P. Foreid, E. Ducla-Soares, Brain Topogr. 11 (1999) 201.